

Cation dynamics in pyridinium nitrate and bis-thiourea pyridinium nitrate inclusion compound studied by  $^2\text{H}$  NMR spectroscopy

This article has been downloaded from IOPscience. Please scroll down to see the full text article.

2007 J. Phys.: Condens. Matter 19 156220

(<http://iopscience.iop.org/0953-8984/19/15/156220>)

View [the table of contents for this issue](#), or go to the [journal homepage](#) for more

Download details:

IP Address: 129.252.86.83

The article was downloaded on 28/05/2010 at 17:40

Please note that [terms and conditions apply](#).

# Cation dynamics in pyridinium nitrate and bis-thiourea pyridinium nitrate inclusion compound studied by $^2\text{H}$ NMR spectroscopy

A Pajzderska, Z Fojud, R Goc and J Wąsicki

Institute of Physics, A Mickiewicz University, Poznań, Poland

Received 14 November 2006, in final form 2 March 2007

Published 26 March 2007

Online at [stacks.iop.org/JPhysCM/19/156220](http://stacks.iop.org/JPhysCM/19/156220)

## Abstract

$^2\text{H}$  NMR (nuclear magnetic resonance) line-shape measurements were performed over a wide temperature range for pyridinium nitrate  $(\text{d}_5\text{PyH})\text{NO}_3$  and bis-thiourea pyridinium nitrate inclusion complex  $\text{T}_2(\text{d}_5\text{PyH})\text{NO}_3$  in order to compare the dynamics of  $\text{d}_5$ -pyridinium cation in both compounds. It was revealed that in both systems the pyridinium cation undergoes reorientations about the axis perpendicular to its plane, among inequivalent potential energy barriers. However, in  $(\text{d}_5\text{PyH})\text{NO}_3$  (no phase transition) the population of the deepest minima decreases monotonically up to the melting point, whereas in  $\text{T}_2(\text{d}_5\text{PyH})\text{NO}_3$  (two phase transitions) this population decreases rapidly in a transition to the high-temperature phase and its value does not depend on temperature. In bis-thiourea pyridinium nitrate inclusion compound the out-of-plane motion of the cation is also found in the intermediate- and high-temperature phases, and the amplitudes of the motion are equal to  $20^\circ$  and  $35^\circ$ , respectively. On the basis of the assumptions of these models, it is possible to reproduce the experimental  $^2\text{H}$  NMR line shapes in an excellent way.

## 1. Introduction

Thiourea forms many inclusion compounds with organic molecules such as carbon tetrachloride [1], chloroform [2], adamantane [3, 4], cycloalkanes [5–8], long branched hydrocarbons [9], substituted benzene rings [10, 11] and some metalorganic compounds [12–15]. The molecules of thiourea are linked by hydrogen bonds  $\text{N}-\text{H}\cdots\text{S}$  into a kind of a honeycomb channel structure in which the guest molecules are located. The diagonal of the channels varies from 0.58 to 0.71 nm. The stoichiometry of these systems is 3:1. Another group of inclusion compounds is made by thiourea with peralkylated ammonium salts [16–18]. The molecules of thiourea and the anions (halogens,  $\text{CO}_2$ ,  $\text{NO}_3$ , benzoic, oxalic and furmanid acids) connected by hydrogen bonds make a complex network of the host. Its shape and size depend on the type of the anion and the length of the peralkylated cation. The stoichiometry of these systems also depends on the type of cation.

Thiourea also forms inclusion compounds with pyridinium salts, of which the systems with bromide [19–21], chloride and iodide [20, 21], nitrate [22, 23] and the system of thiourea with *N*-methylpyridinium iodide [24] are known. The molecules of thiourea form ribbons linked by hydrogen bonds N–H...S. Four such ribbons make a channel of approximately square cross-section, with a diagonal of about 1 nm, containing pyridinium cations or *N*-methylpyridinium cations. The ribbons are not linked by hydrogen bonds. At the sites where the four channels meet there is a smaller channel containing the anion. The cross-section of the channel containing the *N*-methylpyridinium cation is less symmetrical and elongated along the *x* axis so as to accommodate the methyl group. When the halogen anions are replaced with the NO<sub>3</sub> group, we can distinguish two types of wall of the channel made by thiourea ribbons—a flat one and a bent one; moreover, the small channels are losing their channel-like character.

In the majority of structures the host molecules or ions show dynamic and/or conformational disorder. The dynamics of the host molecules in inclusion compounds usually differ from those in pure crystal as a result of a reduction in intermolecular interactions. In molecular systems like thiourea with organic molecules, the main role is played by the van der Waals interactions. In molecular–ionic systems like thiourea with organic salts, the situation is more complex as, apart from the van der Waals interactions, Coulomb interactions and specific interactions such as hydrogen bonds are also of importance. Usually, the dynamics of these complex systems are studied by the solid-state NMR, quasi-elastic neutron scattering (QENS) and molecular dynamics computer simulations (MD).

The aim of this paper is to determine the dynamics of the pyridinium cation in pyridinium nitrate (C<sub>6</sub>D<sub>5</sub>NH)<sup>+</sup>NO<sub>3</sub><sup>−</sup> (denoted hereafter as (d<sub>5</sub>PyH)NO<sub>3</sub>) and in the bis-thiourea pyridinium nitrate inclusion compound [(NH<sub>2</sub>)<sub>2</sub>CS]<sub>2</sub>(C<sub>6</sub>D<sub>5</sub>NH)<sup>+</sup>NO<sub>3</sub><sup>−</sup> (denoted hereafter as T<sub>2</sub>(d<sub>5</sub>PyH)NO<sub>3</sub>). A comparison of the pyridinium cation dynamics in the two compounds is expected to establish the effect of the channels made by thiourea on this dynamics. To the best of our knowledge this is the first attempt at making such a comparison for molecular–ionic systems.

Pyridinium nitrate crystallizes in the monoclinic system, space group *P*2<sub>1</sub>/*c* [25–27]. The ions are linked through the hydrogen bonds N–H...O with a length of 0.276 or 0.31 nm, to form columns along the crystallographic axis *x*. The distances between the pyridinium cations in the column are 0.38 nm at 120 K and 0.39 nm at room temperature. At room temperature the dihedral angle made by the anion and the cation planes was 13.72°, while at 120 K it was 21.12°. In the range 100–389 K this compound does not undergo a phase transition.

The pyridinium cation dynamics in (PyH)NO<sub>3</sub> were studied earlier by NMR. The relaxation time *T*<sub>1</sub> and second moment *M*<sub>2</sub> of the NMR line for protons measured as a function of temperature or pressure [28, 29] have shown that the pyridinium cation undergoes reorientation around the axis perpendicular to its plane, between potential energy barriers of different heights.

In contrast to pyridinium nitrate crystal, in the bis-thiourea pyridinium nitrate inclusion compound the differential scanning calorimetry (DSC) results revealed the occurrence of two phase transitions—one at 216 K and the other at 281 K on heating and at 273 K on cooling [22]. The temperatures of phase transitions determined in [23] on the basis of the dielectric measurements are very similar. The structures of each phase have been established and their sequence is *Pbnm* → *P*2<sub>1</sub>/*c* → *P*2<sub>1</sub> [23]. The pyridinium cations localized in the channels of square cross-sectional area form columns along the crystallographic axis *z*, parallel to the main axis of the channels. The distance between the gravity centres of the pyridinium cations in the column in the low-temperature phase (III) is 0.4176 or 0.4284 nm, in the intermediate phase (II) it is 0.4247 nm, while in the high-temperature phase (I) it is 0.4127 or 0.4134 nm [23]. The angle made by the pyridinium cation plane and the (100) crystal plane

in the high-temperature phase is  $89^\circ$ , in the intermediate phase it is  $63.7^\circ$ , while in the low-temperature phase it is  $64.9^\circ$ . The pyridinium cations and  $\text{NO}_3$  anions in the low-temperature phase and the intermediate phase are linked through the hydrogen bonds  $\text{N-H} \dots \text{O}$ .

Reported in [22], temperature measurements of the relaxation time  $T_1$  and the second moment  $M_2$  of the NMR line for protons performed for the bis-thiourea pyridinium nitrate inclusion compound  $\text{T}_2(\text{PyH})\text{NO}_3$  and its partly deuterated analogues  $\text{T}_2(\text{d}_5\text{PyH})\text{NO}_3$  and  $\text{d}_8\text{T}_2(\text{PyD})\text{NO}_3$  have shown that the pyridinium cation undergoes reorientations about the axis perpendicular to its plane, between inequivalent potential energy barriers, similarly to pyridinium nitrate crystals.

Nuclear magnetic resonance on deuterons has been performed to get more detailed insight into pyridinium cation dynamics in  $(\text{d}_5\text{PyH})\text{NO}_3$  and  $\text{T}_2(\text{d}_5\text{PyH})\text{NO}_3$ . Studies of dynamics by observing proton NMR give more or less averaged information, mainly due to the relatively long distance—up to about 0.6 nm or even 0.8 nm—of dipole–dipole interactions between  $^1\text{H}$  nuclei.

Substitution of protons by deuterium nuclei has a minor influence on the physical properties of the molecule, but all interactions responsible for the NMR line shape for  $^2\text{H}$  take place over a very short distance—of about 0.1 nm. Therefore, one can study the effects of motion of a single molecule which is not masked by intermolecular interactions, as when protons are the probes of motion.

The shape of the NMR absorption line assigned to nuclei with spin  $I = 1$  in a polycrystalline material is determined mainly by the interaction of their quadrupolar moment with the gradient of the electric field surrounding it. Further considerations will be focused on deuterium  $^2\text{H}$ , as this was the resonant nucleus in our experiments.

The dipole–dipole interactions in the case of the  $^2\text{H}$  resonance is very weak, giving a broadening of less than 1 kHz of the NMR line assigned to single crystallites in a powdered sample, so the observed line shape is determined by quadrupolar interactions. The quadrupole moment interaction with the electric field gradient results in a splitting and shifting of the observed NMR line from its central position symmetrically into higher and lower frequencies. For nuclei with spin  $I = 1$ , the NMR line is simply split into a pair of lines symmetrical with respect to the Larmor frequency of this nucleus. The value of this splitting depends on the quadrupolar coupling constant  $Q_{cc}$ , on the components of the tensor representing the electric field gradient and on the relative orientation of the components of this tensor with respect to the direction of the magnetic field  $B_0$ . This splitting is usually two to four orders of magnitude greater than the dipole–dipole broadening. Therefore, it is a quadrupolar interaction which determines the observed NMR line shape.

The description presented above concerns the rigid structure of the material studied. In NMR studies, rigid means that any reorientation of molecules has a frequency much lower than the line width or line splitting in the case of quadrupole interaction. For the materials under study, we can neglect the dipolar interaction as being much smaller than the quadrupolar interaction. Therefore, our further discussions will take into account only the quadrupole interactions.

Any motion of molecules with a sufficiently high frequency leads to narrowing of the quadrupolar splitting. To analyse the experimental data we have written a computer program that calculates the dependence of this splitting on different models of motion of the molecules. We assumed that the frequency of motion is always much higher than the observed splitting.

Talking, for simplicity of description, about the motion of molecules, we in fact consider the motion of nuclei attached to these molecules. The electric field gradient responsible for the splitting of the NMR line arises from the electronic structure of the molecule hosting the nucleus in question. Narrowing of the quadrupole splitting due to the motion of the molecules

is a consequence of averaging of the quadrupole moment of the nucleus interactions with the electric field gradient.

## 2. Experimental details

The compound of  $(d_5\text{PyH})\text{NO}_3$  was obtained by allowing perdeutero-pyridine to react with nitric acid.

The compound  $\text{T}_2(d_5\text{PyH})\text{NO}_3$  was prepared by the dissolution of stoichiometric quantities of thiourea and perdeuterated pyridinium nitrate  $(d_5\text{PyH})\text{NO}_3$ , as described in [22].

All samples were ground to powder, degassed and sealed off under vacuum in glass ampoules for NMR experiments.

The NMR absorption line shape has been recorded for  $^2\text{H}$  using a Bruker DSX 400 spectrometer operating at 61.4 MHz. A standard phase cycled quadrupole echo sequence was used with quadrature detection. The  $\pi/2$  pulse was  $2.4 \mu\text{s}$ ,  $\tau = 15\text{--}40 \mu\text{s}$ . The recorded echo signals were subjected to a fast Fourier transform.

## 3. Results and discussion

### 3.1. The compound of $(d_5\text{PyH})\text{NO}_3$

The  $^2\text{H}$  NMR line was recorded in the range 143–363 K. For the lowest temperatures it is a Pake doublet [30, 31] of widths  $\Delta\nu_{zz} = 265 \text{ kHz}$ ,  $\Delta\nu_{yy} = 141.3 \text{ kHz}$  and  $\Delta\nu_{xx} = 133.5 \text{ kHz}$ . The quadrupole coupling constant  $Q_{cc}$  determined from the line width is 176.7 kHz, while the asymmetry parameter is  $\eta = 0.03$ . These  $Q_{cc}$  and  $\eta$  values are similar to those obtained for  $d_5$ -pyridine [32] and other pyridinium salts  $(d_5\text{PyH})\text{BF}_4$  [33, 34],  $(d_5\text{PyH})\text{ClO}_4$  [35] and  $(d_5\text{PyH})\text{I}$  [36]. The shape of the spectra recorded at a few selected temperatures is presented in figure 1, while the temperature dependences of the line widths  $\Delta\nu_{zz}$ ,  $\Delta\nu_{yy}$  and  $\Delta\nu_{xx}$  are given in figure 2. The line widths  $\Delta\nu_{zz}$  and  $\Delta\nu_{xx}$  decrease monotonically with increasing temperature, and at 363 K they reach the values 127.3 kHz and close to 0 kHz. The width of  $\Delta\nu_{yy}$  only slightly decreases with increasing temperature.

The pyridinium cation dynamics in pyridinium nitrate have already been studied by NMR. Results of temperature and pressure measurements for the relaxation time  $T_1$  and the second moment  $M_2$  of NMR on protons [28, 29] have evidenced that the pyridinium cation undergoes a reorientation around the axis perpendicular to its plane, between potential energy barriers of different height. The results were interpreted by assuming the model of a three-well potential proposed in [37]. In this model, one well is deeper than the other two and the energy difference between the wells is denoted as  $\Delta$ . On the basis of the temperature dependence of  $M_2$ , the temperature changes in  $\Delta$  have been estimated. With increasing temperature,  $\Delta$  decreases, which means that the energy barriers become symmetric. A similar temperature dependence of  $\Delta$  has been reported for other pyridinium salts [38, 39]. Because of the shape of the pyridinium cation, it seems more justified to assume the six-well potential model, with one well deeper than the other five; see figure 3. In this work we assume the six-well potential for interpretation of the temperature dependence of NMR  $^2\text{H}$  for  $(d_5\text{PyH})\text{NO}_3$ . The values of  $\Delta\nu_{zz}$ ,  $\Delta\nu_{yy}$  and  $\Delta\nu_{xx}$  obtained from deuterium lines are proportional to the corresponding three components of the electric field gradient,  $V_{zz}$ ,  $V_{yy}$  and  $V_{xx}$ . As the component  $\Delta\nu_{yy}$  depends only insignificantly on temperature, we assume that  $V_{yy}$  is perpendicular to the pyridinium cation plane. The  $V_{zz}$  component lies along the C–D bond and the  $V_{xx}$  component is perpendicular to it. Following the procedure described in [36], the ratio of the  $z$  component of the electric field gradient averaged as a result of the reorientations of the pyridinium cation,  $V'_{zz}$ , to the value of this component

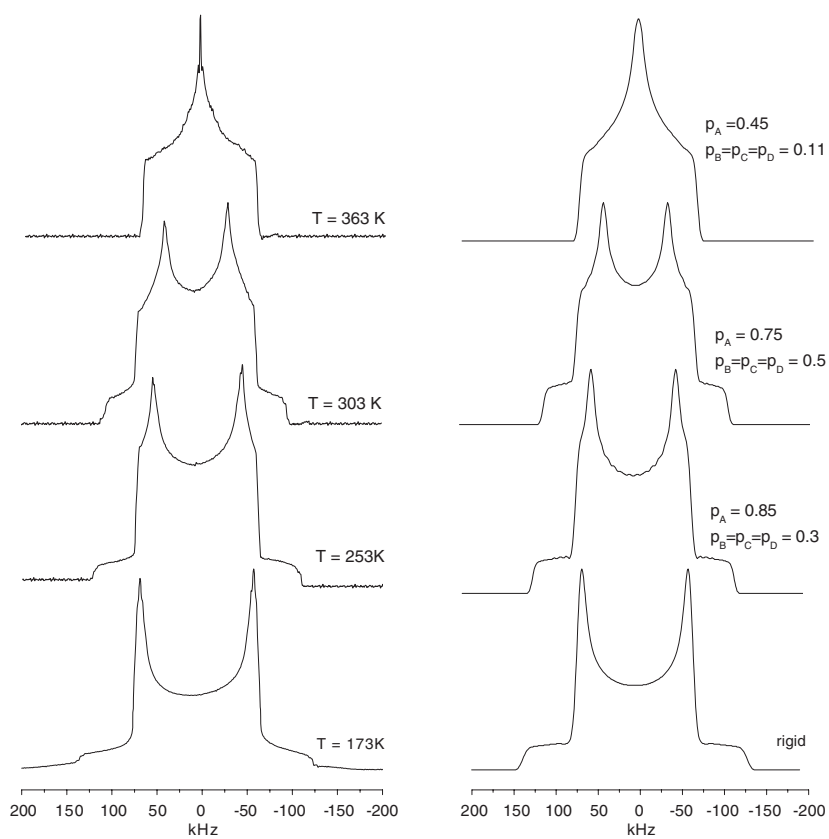


**Figure 1.** Experimental (left) and simulated (right)  $^2\text{H}$  NMR line shape for  $(\text{d}_5\text{PyH})\text{NO}_3$ .

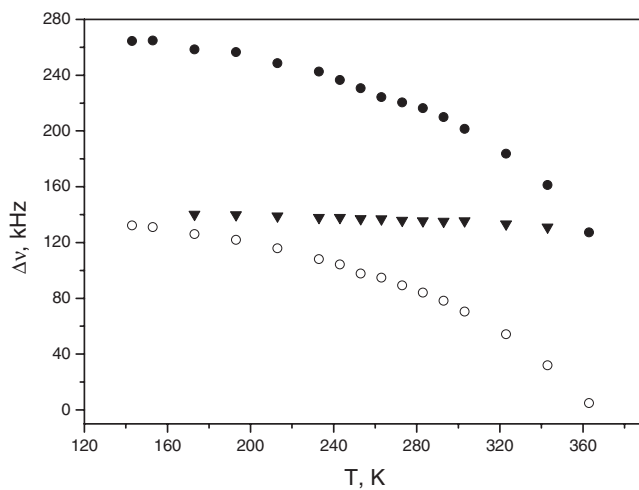


**Figure 2.** Temperature dependence of the line widths (●)  $\Delta\nu_{zz}$ , (▼)  $\Delta\nu_{yy}$  and (○)  $\Delta\nu_{xx}$  for  $(\text{d}_5\text{PyH})\text{NO}_3$ .

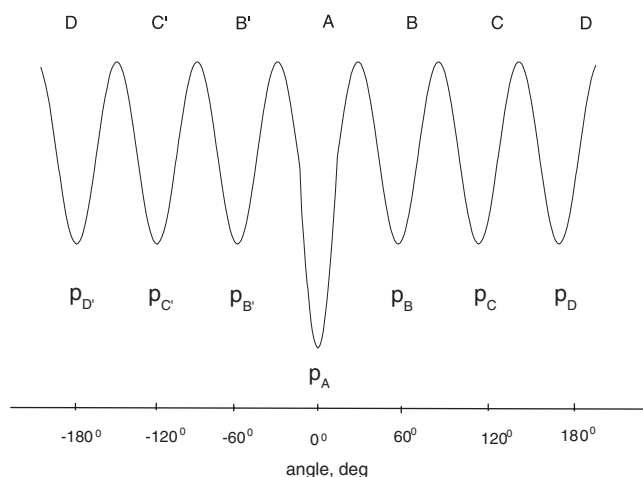


**Figure 3.** The shape of the potential for pyridinium cation reorientation.

for the rigid lattice,  $V_{zz}$ , can be expressed in terms of  $a = \exp(-\Delta/RT)$ . For the six-well potential model the authors of [33] derived the following expression for  $(V'_{zz}/V_{zz})$ :

$$(V'_{zz}/V_{zz}) = (a + 2)/2(1 + 5a). \quad (1)$$

Therefore, the temperature dependence of the parameter  $a$  and thus the probability of population of particular potential energy minima can be obtained from the line width of  $^2\text{H}$  NMR. For the six-well potential model the populations of the potential energy minima are calculated from [33]:

$$p_A = 1/(1 + 5a), \quad p_B = p_{B'} = p_C = p_{C'} = p_D = a/(1 + 5a). \quad (2)$$

Knowing the populations of particular potential energy minima as a function of temperature, it is possible to perform simulations of the deuteron spectra, which have been made with the program described in [33]. The program presented there was designed in such a way that consecutive positions of the resonant nuclei connected with the reorienting molecule were in the plane of the molecule, because the axis of this molecule reorientation was perpendicular to its plane. It was assumed that the molecule can make  $60^\circ$  jumps about its  $C'_6$  axis, perpendicular to the plane of the molecule. So there are six positions that can be taken by the molecule. Each of these positions can be occupied with a probability from 0 to 100. Assigning the probability 100 to one position and zeros to five others means a rigid structure—no jumps. By assigning different probabilities (from 0 to 100) to different positions of the molecule, we can simulate unequal barriers, hindering the reorientation about the  $C'_6$  axis.

The general flow of calculation in our computer program is as follows:

- (1) The quadrupolar constant  $Q_{cc}$  and the asymmetry parameter  $\eta$  are given.
- (2) The line splitting is calculated for the rigid structure and for an arbitrary initial orientation of the single-crystal sample with respect to the direction  $B_0$ .
- (3) Calculations are repeated for a random distribution of crystallites in a powdered sample, giving as a result the line shape for the rigid polycrystalline sample.
- (4) The program calculates the quadrupolar interaction for all positions of the molecule resulting from the assumed model of the reorientation and takes the average value to find the NMR line splitting.

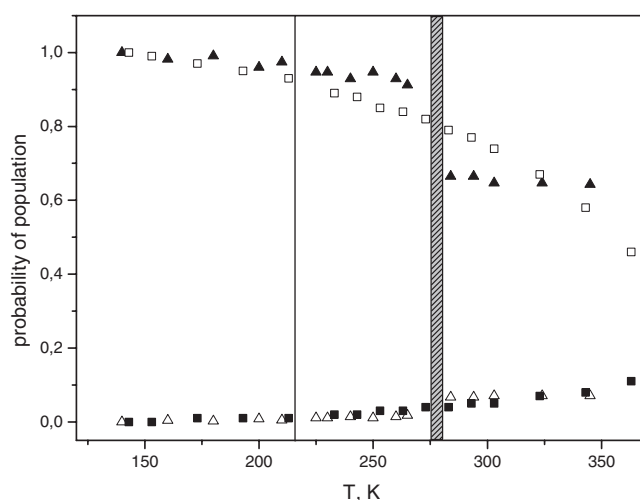


**Figure 4.** The temperature dependence of the probability of populations for  $(d_5\text{PyH})\text{NO}_3$ : ( $\square$ )  $p_A$ , ( $\blacksquare$ )  $p_B = p_C = p_D$  and  $T_2(d_5\text{PyH})\text{NO}_3$ : ( $\blacktriangle$ )  $p_A$ , ( $\triangle$ )  $p_B = p_C = p_D$ . The phase transition temperatures pointed out here relate to  $T_2(d_5\text{Py})\text{NO}_3$ .

- (5) The results of the calculation from (4) are averaged over the spatial distribution of crystallites in a powdered sample.

A good agreement between the simulated and experimental lines obtained for selected temperatures is illustrated in figure 1. Figure 4 gives the temperature dependence of the probability of population of particular potential energy minima. The probability of population of the deep minimum  $p_A$  decreases monotonically with increasing temperature from 1 at 143 K to 0.45 at 363 K. Hence, it can be concluded that, with increasing temperature, the potential energy barriers undergo a process of symmetrization but, even for the highest temperatures for which the measurements were made (20 K lower than the melting point), the barriers are not fully symmetric.

### 3.2. The inclusion compound $T_2(d_5\text{PyH})\text{NO}_3$

$^2\text{H}$  NMR line-shape measurements for the bis-thiourea pyridinium nitrate inclusion compound were performed for the range 140–350 K. Figure 5 presents the selected spectra that are typical for each phase. For each spectrum the temperature dependences of the line widths  $\Delta\nu_{xx}$ ,  $\Delta\nu_{yy}$  and  $\Delta\nu_{zz}$  are presented in figure 6. In the low-temperature phase (phase III) the spectrum is described well by a typical Pake doublet, and its widths at 140 K are  $\Delta\nu_{zz} = 254$  kHz,  $\Delta\nu_{yy} = 138$  and  $\Delta\nu_{xx} = 126$  kHz. The quadrupole coupling constant  $Q_{cc}$  calculated from the line width is 169.3 kHz, while the asymmetry parameter  $\eta$  is 0.05. The quadrupole coupling constant  $Q_{cc}$  is lower than that obtained for pyridine- $d_5$  [32] or for the pyridinium cation in other pyridinium salts [33–35]. The parameter of asymmetry in the complex that is studied is slightly higher than in pyridine- $d_5$  [32] or in the other pyridine salts [33–35]. The line width decreases monotonically with increasing temperature up to  $\Delta\nu_{zz} = 248$  kHz,  $\Delta\nu_{yy} = 135$  and  $\Delta\nu_{xx} = 120$  kHz at 210 K. The line shape observed in phase II is very similar to that recorded in the low-temperature phase. The line widths of  $\Delta\nu_{xx}$  and  $\Delta\nu_{yy}$  in phase II only slightly change with increasing temperature: from 114 kHz and 132 kHz at 225 K to 106 kHz and 124 kHz at 265 K. The width of  $\Delta\nu_{zz}$  decreases monotonically from 240 kHz at 225 K



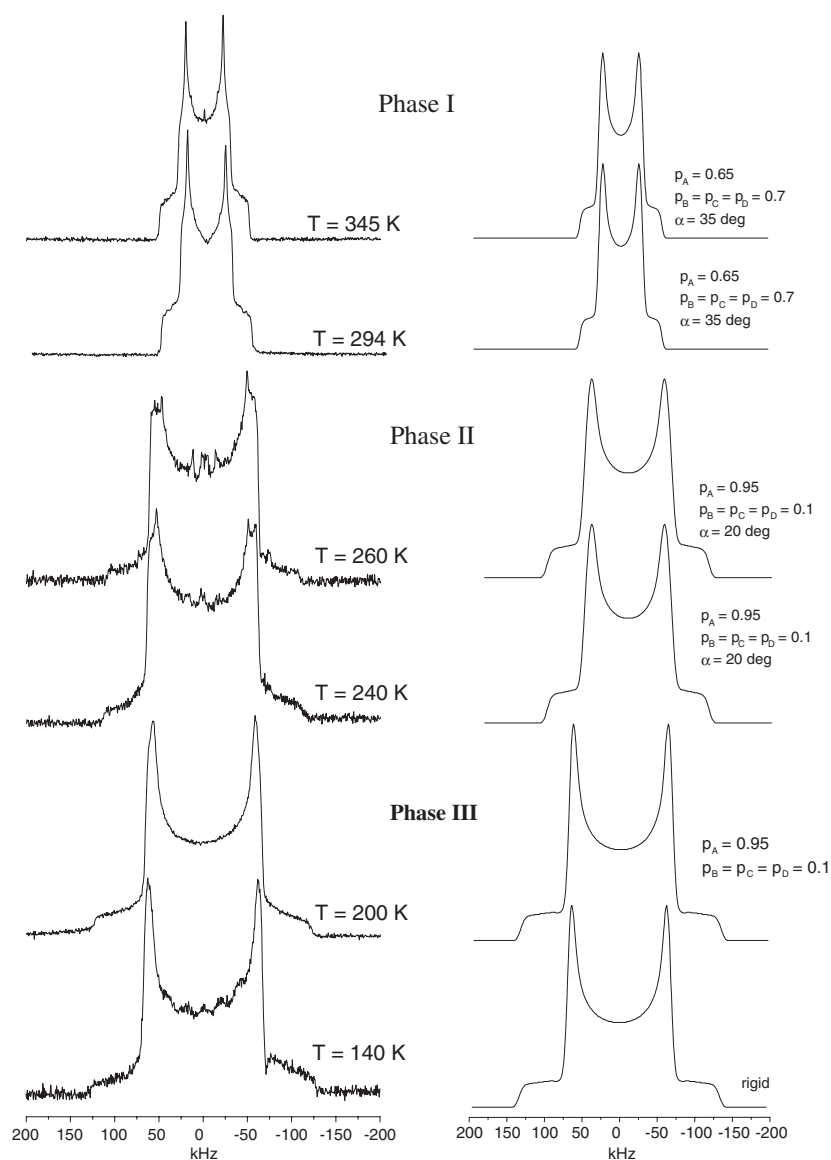


**Figure 5.** Experimental (left) and simulated (right)  $^2\text{H}$  NMR line shape for  $\text{T}_2(\text{d}_5\text{PyH})\text{NO}_3$ .

to 218 kHz at  $T = 265$  K. At the phase transition from II to I phase, the shape of the line changes and the widths of  $\Delta v_{zz}$ ,  $\Delta v_{yy}$  and  $\Delta v_{xx}$  undergo jumpwise changes. In phase I these widths are 105, 64 and 50 kHz, and the shape of the line does not depend on temperature. A recent dielectric spectroscopy study has revealed pyridinium cation reorientations in phase III of  $\text{T}_2(\text{PyH})\text{NO}_3$  [23]. As follows from NMR measurements on protons, the reorientations occur between inequivalent potential energy barriers [22]. This conclusion is confirmed by the shape of the line and a small change in its width in phase III. It seemed interesting to check the effect of the phase transitions on the cation reorientations in phases II and I.

In analogy to  $(\text{d}_5\text{PyH})\text{NO}_3$ , the cation was assumed to reorient about the pseudo-hexagonal  $C'_6$  axis perpendicular to its plane, in the potential with six minima separated by  $60^\circ$ , with

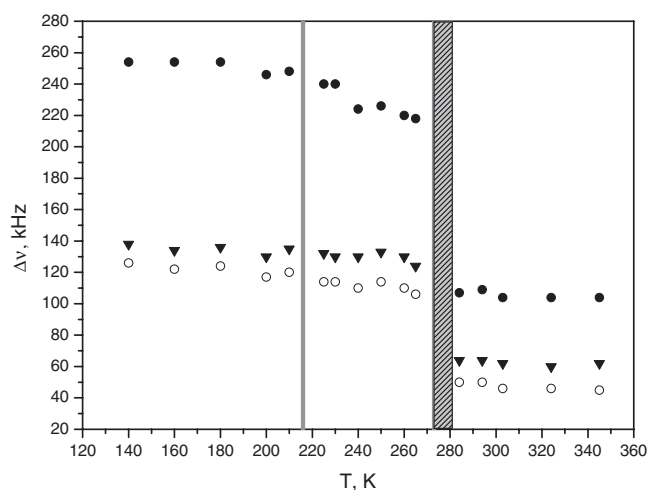


**Figure 6.** Temperature dependence of the linewidths ( $\bullet$ )  $\Delta v_{zz}$ , ( $\blacktriangledown$ )  $\Delta v_{yy}$  and ( $\circ$ )  $\Delta v_{xx}$  for  $T_2(d_5\text{PyH})\text{NO}_3$ . The vertical solid lines indicate the phase transitions.

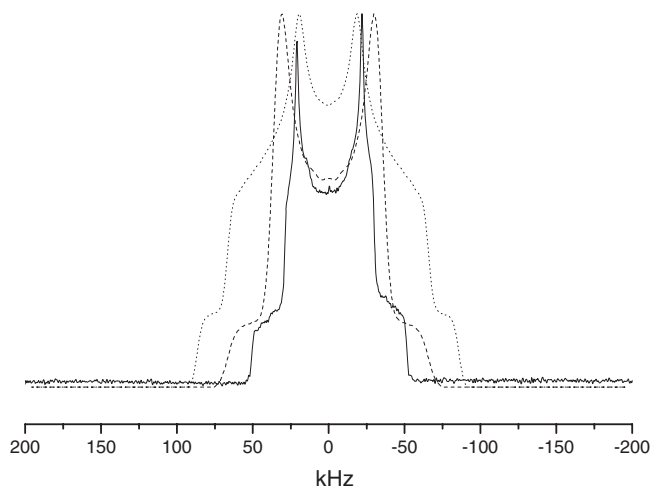


**Figure 7.** Experimental  $^2\text{H}$  spectrum at 303 K (solid line) and simulation: - - - equivalent barrier,  $\cdots\cdots p_A = 0.60$ ,  $p_B = p_C = p_D = 0.8$ .

one deeper than the other five (figure 3). Similarly to that for  $(d_5\text{PyH})\text{NO}_3$ , the probability of population of each potential energy minimum in each phase was calculated from the temperature dependence of the line width  $\Delta v_{zz}$ , equations (1) and (2). On the basis of these probabilities, using the program described above, the line shapes were simulated for three phases. The simulated line reproduces the experimental line well only in the low-temperature phase III. But the widths  $\Delta v_{xx}$ ,  $\Delta v_{yy}$  and  $\Delta v_{zz}$  of the experimental spectra in phases II and I are much smaller than the simulated widths. In phase I, the experimental widths are also narrower than the widths simulated for the cation reorientation over equivalent barriers (figure 7).

This means that the cation will have to perform an additional reorientation, and a significant change in  $\Delta v_{yy}$  indicates the out-of-plane character of the motion. Ripmeester *et al* in their

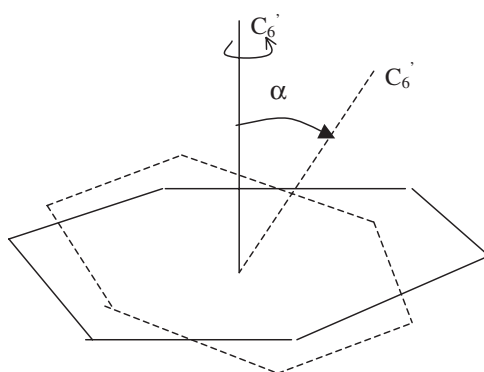


**Figure 8.** Schematic drawing of the pyridinium cation motion.

paper [40] described an analogous situation and, to obtain satisfactory averaging of quadrupolar interactions, they introduced two extra modes of motion—jumps of the molecule about two perpendicular axes, lying in the plane of the molecule. These additional motions, superimposed on the previously described motion, give good agreement between the measured and simulated NMR line shapes for deuterons. For the compound that we studied, it was assumed that the  $C'_6$  axis was tilted by a certain angle  $\pm\alpha$ , so that the cation's ring also performed an out-of-plane reorientation between two positions (figure 8). This assumption required modification of the computer program, adding an additional mode of motion—about an axis lying in the plane of the molecule. We added only one axis as, from the symmetry of the molecule under study, it follows that there are two equivalent axes passing through two deuterons located on opposite sides of the pyridinium cation and one axis passing through a deuteron and a proton also situated on opposite sites of the pyridinium cation.

Justification for simulating jumps about only one axis in the plane of the molecule is as follows. The NMR line shape recorded on deuterons is a function of the electric field gradient nearest to it. The interaction between deuterons is negligible and the influence of one proton per molecule on the deuteron line shape is also a few orders of magnitude smaller than the quadrupolar interaction determining the line shape.

Therefore, we assumed, and checked in the preliminary simulations, that reorientation about one axis, chosen from the three possible axes described above, regardless of the position of this axis, gives satisfactory results in simulating the NMR line shape for this compound.

NMR line shapes obtained with such a model of motion incorporated into the new version of the computer program were in good agreement with the experimental data, so the necessity to simulate jumps about two extra axes, as in Ripmeester's analysis, was abandoned [40].

A comparison of the experimental lines with those simulated assuming that the pyridinium cation performs two types of motion (in-plane reorientations among six positions and out-of-plane reorientations among two positions) is presented in figure 5. A combination of the two types of reorientations provided a very good reproduction of the experimental lines recorded in phases II and I. The in-plane motion about the axis perpendicular to the cation's plane is characterized by the probabilities of population of each potential energy minimum. The temperature changes in the probability of population  $p_A$  of the deepest minimum and in the population  $p_B (= p_C = p_D)$  of other minima are presented in figure 4. In the low-temperature and intermediate phases, the probability  $p_A$  decreases monotonically from 1 at 140 K to 0.91 at 265 K, and the transition between these phases has an insignificant effect on it. The situation is different at the transition between the intermediate and the high-temperature phase, at which

a jump change in the probability is observed ( $p_A = 0.65$ ). In the high-temperature phase its value does not depend on temperature. The out-of-plane motion takes place in the intermediate phase ( $\alpha = 20^\circ$ ) and the high-temperature phase ( $\alpha = 35^\circ$ ). As only deviations greater than  $15^\circ$  can significantly modify the line shape, the occurrence of out-of-plane reorientations, but of smaller amplitude, cannot be excluded in the low-temperature phase. A small narrowing of the line  $\Delta v_{yy}$  with increasing temperature observed for pyridinium nitrate can suggest the cation's out-of-plane deviations, but their amplitude must surely be smaller than  $15^\circ$ .

The pyridinium cations located in the channels made by the thiourea molecules sweep a much greater volume (as they reorient in-plane and out-of-plane) than the cations in pure pyridinium nitrate (reorienting only in-plane). Out-of-plane motion of the cation in  $T_2(d_5\text{PyH})\text{NO}_3$  is possible, as the distances between the cations in the columns are greater than in  $(d_5\text{PyH})\text{NO}_3$ . Therefore, it can be concluded that, in the inclusion compound studied, the cations have more freedom of reorientation than in pure crystal.

As no other examples of comparisons of cation dynamics in pure crystal and inclusion compounds have been found in the literature, we cannot conclude whether our result is typical of ion–molecular systems. However, similar studies have been performed for molecular compounds. It has been found that molecules of benzene placed in 1,3-cyclohexanedione cyclamer perform the same molecular reorientations as in the pure crystal—that is, reorientational jumps about the  $C_6$  axis perpendicular to the ring's plane and out-of-plane librations of the rigid ring—the so-called wobbling [41]. However, the energy barrier for the benzene molecule jumps about the  $C_6$  axis in cyclamer is higher than that in pure benzene by  $8.5 \text{ kJ mol}^{-1}$ . The pyridine molecules in tri-*o*-thymotide (TOT) perform (i) in-plane reorientation among inequivalent energy barriers (restricted in-plane), (ii)  $180^\circ$  jumps about the two-fold axis, and (iii) out-of-plane librations of a rigid ring [40]. In the pure crystal the pyridine molecules do not perform any reorientations in the NMR time scale up to its melting point [40]. The molecules of benzene and pyridine in the host–guest compounds of *p*-tert-butylcalix[4]arene inclusion compound show complex dynamics. Benzene undergoes in-plane rotation followed by reorientation about the compound's four-fold axis of symmetry. Pyridine reorients about the pyridine  $C_2$  molecular symmetry axis, followed by guest reorientation about the compound's four-fold axis of symmetry [42].

Molecules of pyridine in pyridine- $d_5$ -tris-(1,2-dioxyphenyl)-cyclotriposphazene inclusion compound have much freedom of movement. In [43] the authors have proposed a combined rotation on the cone–small-angle fluctuation model, which assumes a fast molecular reorientation between two superimposed cones, with an opening angle for the inner cone of between  $59^\circ$  and  $73^\circ$ .

In the pure 1,4-di-*tert*-butylbenzene crystal the phenyl ring is rigid, in contrast to the methyl or *tert*butyl groups [10]. In the 1,4-di-*tert*-butylbenzene molecule in the inclusion compound with thiourea, the phenyl ring also performs reorientations, besides the methyl and *tert*butyl groups [10, 11].

#### 4. Conclusions

Results of the  $^2\text{H}$  NMR study performed for  $(d_5\text{PyH})\text{NO}_3$  and  $T_2(d_5\text{PyH})\text{NO}_3$  have shown that, in both systems, the pyridinium cation undergoes reorientations about the axis perpendicular to its plane, among inequivalent potential energy barriers. The probability of population of the deep potential energy minimum  $p_A$  decreases monotonically with increasing temperature in  $(d_5\text{PyH})\text{NO}_3$  up to the melting point and in  $T_2(d_5\text{PyH})\text{NO}_3$  only in phases III and II. At the phase transition from II to I, the probability  $p_A$  in  $T_2(d_5\text{PyH})\text{NO}_3$  jumps, and its value no longer depends on temperature. In  $T_2(d_5\text{PyH})\text{NO}_3$ , the out-of-plane motion of the cation

is also observed in phases II and I, and the amplitude of this motion is equal to  $20^\circ$  and  $35^\circ$ , respectively.

### Acknowledgment

The work has been financed by the Ministry of Science and Higher Education from the 2006–2008 funds, grant no. N202 134 31/2331.

### References

- [1] Fait J J, Fitzgerald A, Caughlan C N and McCandless F P 1991 *Acta Crystallogr. C* **47** 332
- [2] Chekhova G N, Shubin Yu V, Mesyats E A, Pinakov D V, Logvinenko V A and Zelenin yu M 2005 *Russ. J. Phys. Chem.* **79** 1017
- [3] Gopal R, Robertson B E and Rutherford J S 1989 *Acta Crystallogr. C* **45** 257
- [4] Greenfield M S, Ronemus A D, Vold R L, Vold R R, Ellis P D and Raidy T R 1987 *J. Magn. Reson.* **72** 89
- [5] Clement R, Jedouez J and Mazieres C 1974 *Solid State Chem.* **10** 46
- [6] Poupko R, Furman E, Muller K and Luz Z 1991 *J. Phys. Chem.* **95** 407
- [7] MacIntosh M R, Fraser B, Gruwel M L H, Wasylshen R E and Cameron T S 1992 *J. Phys. Chem.* **96** 8572
- [8] Maris T, Henson M J, Heynes S J and Prout K 2001 *Chem. Mater.* **13** 2483
- [9] Harris K D M 1996 *J. Mol. Struct.* **374** 241
- [10] Penner G H, Polson J M, Stuart C, Ferguson G and Kaitner B 1992 *J. Phys. Chem.* **96** 5121
- [11] Sidhu P S, Penner G H, Jeffrey K R, Zhao B, Wang Z L and Goh I 1997 *J. Phys. Chem. B* **101** 9087
- [12] Clement R, Claude R and Mazieres C 1974 *J. Chem. Soc. Chem. Commun.* **16** 654
- [13] Hough E and Nicholson D G 1978 *J. Chem. Soc. Dalton Trans.* **1** 15
- [14] Tam W, Eaton D F, Calabrese J C, Williams I D, Wang Y and Anderson A G 1989 *Chem. Mater.* **1** 128
- [15] Heyes S J, Clayden N J and Dobson C M 1991 *J. Phys. Chem.* **95** 1547
- [16] Li Q and Mak T C W 1996 *Acta Crystallogr. B* **52** 989
- [17] Li Q and Mak T C W 1997 *Acta Crystallogr. B* **53** 252
- [18] Li Q and Mak T C W 1999 *J. Incl. Phenom.* **35** 621
- [19] Truter M R and Vickery B L 1978 *Acta Crystallogr. B* **28** 387
- [20] Prout K, Heyes S J, Dobson C M, McDaid A, Maris T, Muller M and Szaman M J 2000 *Chem. Mater.* **12** 3561
- [21] Grottel M, Pajzderska A and Wąsicki J 2004 *Z. Naturf. a* **58** 638
- [22] Grottel M, Kozak A, Pajzderska A, Szczepański W and Wąsicki J 2004 *Z. Naturf. a* **59** 505
- [23] Małuszyńska H and Czarnecki P 2006 *Z. Kristallogr.* **221** 218
- [24] Pajzderska A, Małuszyńska H, Grottel M, Gdaniec M and Wąsicki J 2006 *Mol. Phys.* **104** 1819
- [25] Serewicz J A, Robertson B K and Meyers E A 1965 *J. Phys. Chem.* **69** 1915
- [26] Batsanov A S 2004 *Acta Crystallogr. E* **60** 02424
- [27] Batsanov A S 2004 *Acta Crystallogr. E* **6** 002426
- [28] Kozak A, Grottel M, Wąsicki J and Pająk Z 1994 *Phys. Status Solidi a* **143** 65
- [29] Lewicki S, Wąsicki J, Bobrowicz-Sarga L, Pawlukoje A, Natkaniec I and Kozak A 2003 *Phase Transit.* **76** 261
- [30] Cohen M H and Reif F 1957 *Solid State Phys.* **5** 321
- [31] Barnes R G 1974 *Adv. Nucl. Quadr. Reson.* **72** 89
- [32] Barnes R G and Bloom J W 1972 *J. Chem. Phys.* **57** 3082
- [33] Fojud Z, Goc R, Jurga S, Kozak A and Wąsicki J 2003 *Mol. Phys.* **101** 1469
- [34] Beck B, Villanueva-Garibay J A, Muller K and Roduner E 2003 *Chem. Mater.* **15** 173
- [35] Vujosevic D, Muller K and Roduner E 2006 *J. Phys. Chem. B* **110** 8598
- [36] Ripmeester J 1986 *J. Chem. Phys.* **85** 747
- [37] Ito Y, Asaji T and Nakamura D 1988 *Ber. Bunsenges. Phys. Chem.* **92** 885
- [38] Kozak A, Wąsicki J and Pająk Z 1996 *Phase. Transit.* **57** 153
- [39] Wąsicki J, Kozak A, Pająk Z, Czarnecki P, Belushkin A V and Adams M A 1996 *J. Chem. Phys.* **105** 9470
- [40] Facey G A, Ratcliffe C I and Ripmeester J A 1995 *J. Phys. Chem.* **99** 12249
- [41] Ok J H, Vold R R and Vold R L 1989 *J. Phys. Chem.* **93** 7618
- [42] Bouwer E B, Enright G D, Ratcliffe C I, Facey G A and Ripmeester J A 1999 *J. Phys. Chem.* **103** 10604
- [43] Villanueva-Garibay J A and Muller K 2006 *Phys. Chem. Chem. Phys.* **8** 1394